Supplementary information

METHODS SUMMARY

Major elements: Major element analyses of silicate minerals were carried out in the GEMOC Key Centre at Macquarie University using a Cameca SX50 electron microprobe (EMP). The EMP was equipped with five crystal spectrometers, and an accelerating voltage of 15 kV and a sample current of 20 nA were used for the analyses. The width of the electron beam was 5 μm. Standards were well-characterized natural and synthetic materials (e.g. forsterite, chromite, wollastonite, kyanite, albite, rutile, hematite, spessartine, orthoclase, zircon, Y-Al garnet, Hf metal) and matrix corrections were performed following the method of Pouchou and Pichoir (1984). Counting time was 10 s for peaks and 5 s for background on either side of the peak. Accuracy and precision are better than ±0.5 wt.% for major elements.

Clinopyroxene Sr–Nd–Hf isotopes: Strontium, Nd, and Hf isotope compositions of cpx separates from the peridotite xenoliths were determined at the State Key Laboratory of Lithospheric Evolution, Institute of Geology and Geophysics, Chinese Academy of Sciences. The mineral separates were washed with ultra-pure (Milli-Q) water, and ground to 200–400 mesh using an agate mortar before isotopic analysis. About 150–300 mg of cpx powder was weighed into 7 ml SavillexTM Teflon beakers, and appropriate amounts of mixed ^{87}Rb–^{84}Sr, ^{149}Sm–^{150}Nd, ^{176}Lu, and ^{180}Hf spikes were added. Analytical details for sample digestion and column separation procedures are described by Chu et al. (2009).

The Rb–Sr and Sm–Nd isotopic analyses were conducted using a Finnigan MAT 262 thermal ionization mass spectrometer. Measured ^{87}Sr/^{86}Sr and ^{143}Nd/^{144}Nd ratios were corrected for mass-fractionation using ^{86}Sr/^{88}Sr = 0.1194 and ^{146}Nd/^{144}Nd = 0.7219, respectively. During the period of data collection, the measured values for the NBS-987 Sr standard and the JNdi-1 Nd standard were ^{87}Sr/^{86}Sr = 0.710245 ± 16 ($2\sigma_n$, n = 6) and ^{143}Nd/^{14}4Nd = 0.512117 ± 10 ($2\sigma_n$, n = 6), respectively. Lutetium and Hf were measured using a ThermoElectron Neptune multi-collector ICP-MS system. Hafnium isotopic ratios were normalized to ^{179}Hf/^{177}Hf = 0.7325 and ^{176}Lu/^{175}Lu isotopic ratios were normalized using Yb isotopic ratios. During the analytical campaign, an Alfa Hf

standard was measured 10 times and the average value of $^{176}Hf/^{177}Hf$ was 0.282179 ± 4 (2σ).

Whole rock Re–Os and PGE analyses: whole rock Re–Os isotopic compositions and PGE abundances were determined at both the State Key Laboratory of Lithospheric Evolution, Institute of Geology and Geophysics, Chinese Academy of Sciences (IGGCAS) and the Isotope Geochemistry Laboratory, University of Maryland (UMD).

The methods used at both laboratories are similar to those described by Shirey & Walker (1995), and Walker et al. (2008). Rhenium, Os, Ir, Ru, Pt, Pd concentrations and Os isotopic compositions were obtained from the same Carius tube sample digestion (for details of Re–Os and PGE chemistry see Walker et al., 2002, 2008 and Chu et al., 2009).

Osmium isotopic compositions were measured by negative thermal ionization using either a GV Isoprobe-T mass spectrometer at IGGCAS (Chu et al., 2009), or a VG Sector 54 mass spectrometer at UMD (Walker et al., 2002, 2008). For these measurements, purified Os was loaded onto platinum filaments and $Ba(OH)_2$ was used as an ion emitter. At IGGCAS, all samples were run in static mode using Faraday cups. At UMD, samples were run in static mode on Faraday cups, or in peak-jumping mode with a single electron multiplier, depending on the amount of Os. The measured Os isotopic ratios were corrected for mass fractionation using $^{192}Os/^{188}Os = 3.0827$. The in-run precisions for Os isotopic measurements were better than ±0.2% (2RSD) for all the samples. During the period of measurements of our samples, the $^{187}Os/^{188}Os$ ratio of the Johnson–Matthey standard of UMD was 0.11380 ± 4 ($2\sigma_n$, n = 3) at IGGCAS, and 0.11379 ± 2 ($2\sigma_n$, n=3) for Faraday cups and 0.1138 ± 1 ($2\sigma_n$, n = 3) for electron multiplier at UMD.

The isotope dilution analyses of Re, Ir, Ru, Pt, and Pd were conducted either at IGGCAS and UMD using a Thermo-Electron Neptune MC-ICP-MS system with an electron multiplier in peak-jumping mode or using Faraday cups in static mode, according to the measured signal intensity, or at UMD using a Nu-Plasma MC-ICP-MS system with a triple electron multiplier configuration in static mode. Mass fractionations (and gain effects of different multipliers for the UMD method) for Re, Ir, Ru, Pt, and Pd were corrected using Re, Ir, Ru, Pt and Pd standards that were interspersed with the samples. In-run precisions for $^{185}Re/^{187}Re$, $^{191}Ir/^{193}Ir$, $^{194}Pt/^{196}Pt$, $^{105}Pd/^{106}Pd$, and $^{99}Ru/^{101}Ru$ were typically 0.1–0.3% (2RSD).

In-situ Re-Os and PGE analysis of sulfides: The analytical procedures for in situ Re-Os isotopic analysis have been described in detail by Pearson et al. (2002) (also see www.es.mq.edu.

au/GEMOC). Analyses were carrried out using a Merchantek LUV266 laser microprobe with a modified ablation cell, attached to a Nu Plasma multicollector ICPMS. All ablations were carried out using He as the carrier gas, to enhance sensitivity and reduce elemental fractionation. Most analyses were carried out at 4 Hz repetition rate and laser energies of 1–2 mJ/pulse, and typical pit diameters were 50–80 microns. A dry aerosol of Ir, produced by a CETAC MCN6000 desolvating nebuliser, was bled into the gas line between the ablation cell and the ICPMS to provide a mass-bias correction with a precision independent of the abundance of Os in the sample. Masses 188–194 were measured in Faraday cups, and masses 185 and 187 were measured in ETP ion counters. The ion counters were calibrated initially against the Faraday cups and one another using a two-cycle analysis of a standard Os solution, rather than the sequential analysis of Ir + Os and Re + Ir solutions used by Pearson et al. (2002). During ablation runs, a standard NiS bead with 200 ppm Os and Pt (PGE-A) was analyzed between samples, to monitor and correct any drift in the ion counters. These corrections typically were less than 1% over a long day's analytical session. The overlap of ^{187}Re on ^{187}Os was corrected by measuring the ^{185}Re peak and using ^{187}Re/^{185}Re = 1.6741, as described by Pearson et al. (2002). The precision and accuracy of the method are discussed in detail by Pearson et al. (2002). Under ideal circumstances (i.e. sulfides ~50 microns in diameter, and containing at least 40 ppm Os), an internal precision for ^{187}Os/^{188}Os of 0.1–0.3% (2SE) is routinely obtained; for smaller grains or lower Os contents (<5–10 ppm), an internal precision of 1–2% is routine. The external reproducibility of ^{187}Os/^{188}Os for the PGE-A standard over several months is ±0.00048 (2sd), and the mean value of ^{187}Os/^{188}Os is indistinguishable from that derived by TIMS analysis.

In situ PGE analyses were performed with the GEMOC LAM-ICP-MS (Alard et al., 2000). The six PGE, Au, and Se were determined with a custom-built laser ablation system linked to a Perkin-Elmer Sciex ELAN 6000 ICP-MS (RF power, 1050 W). The laser is a Continuum Surelite I-20 Q-switched quadrupled frequency Nd: YAG laser delivering a 266-nm ultraviolet beam. Ablation was done in a pure He atmosphere (0.85L/min). Analytical conditions included a 40- to 60-mm beam diameter, 4 Hz laser frequency, and a beam energy ~0.5 mJ/pulse. Raw data were processed on line by means of the GLITTER software package (Van Achterbergh et al., 1999). ^{63}Cu^{40}Ar interference on ^{103}Rh (monoisotopic) was corrected by ablating a pure Cu metal several times during the run and determining the production rate of ^{63}Cu^{40}Ar. The accuracy of the

correction is checked by correcting ^{105}Pd for $^{65}Cu^{40}Ar$ interference and comparing it to ^{106}Pd, which is free of major interference, except for $^{66}Zn^{40}Ar$. However, Zn abundance in mantle sulfide is generally low <0.3 wt%. A quenched NiS bead doped with PGE and several other chalcophile elements was used as external standard. The similarity of matrix between the standard and the analyzed sulfide allows a straightforward processing of the data (Ballhaus and Sylvester, 2000). The homogeneity of the standard is attested by long-term reproducibility (Alard et al., 2000). Typical detection limit, for the conditions described above, are lower than 40 ppb for all PGE but Ru, which showed a 70 ppb detection limit. Detailed procedure was described by Alard et al. (2000).

References:

Alard, O., Griffin, W. L., Lorand, J. P., Jackson, S. E., O'Reilly, S. Y., Non-chondritic distribution of the highly siderophile elements in mantle sulfides. Nature, 407, 891–894 (2000).

Chu, Z.-Y., Wu, F.-Y., Walker, R. J., Rudnick, R. L., Pitcher, L., Puchtel, I. S., Yang, Y.-H., Wilde, S. A. Temporal Evolution of the Lithospheric Mantle beneath the Eastern North China Craton. Journal of Petrology 50, 1857-1898 (2009).

Pearson, N. J., Alard, O., Griffin, W. L., Jackson, S. E., O'Reilly, S. Y. In situ measurement of Re-Os isotopes in mantle sulfides by laser ablation multi-collector inductively-coupled mass spectrometry: Analytical methods and preliminary results. Geochim. Cosmochim. Acta, 66, 1037–1050 (2002).

Pouchou, J. L., Pichoir, F. A new model for quantitative X-ray microanalysis. Part 1: application to the analysis of homogeneous samples. Rech. Aerosp. 5, 13–38 (1984).

Van Achterberg E., Ryan C. G., Griffin W. L. GLITTER: On line intensity reduction for the laser ablation inductively coupled plasma mass spectrometry. In 9th Goldschmidt Conference, pp. 305. Boston, MA. J. Conf. Abstract, Cambridge, S (1999).

Shirey, S. B., Walker, R. J. Carius tube digestions for low-blank rhenium–osmium analysis. Analytical Chemistry 67, 2136–2141 (1995).

Walker, R. J., McDonough, W. F., Honesto, J., Chabot, N. L., McCoy, T. J., Ash, R. D., Bellucci, J. J. Modeling fractional crystallization of group IVB iron meteorites. Geochimica et Cosmochimica Acta 72, 2198–2216 (2008).

Walker, R. J., Prichard, H. M., Ishiwatari, A., Pimentel, M. The osmium isotopic composition of convecting upper mantle deduced from ophiolite chromites. Geochimica et Cosmochimica Acta 66, 329–345 (2002).

Supplementary data

Table DR1. Rb-Sr isotopic data of phlogopites in the kimberlite from the North Korea

No	Rb [ppm]	Sr [ppm]	$^{87}Rb/^{86}Sr$	$^{87}Sr/^{86}Sr$	2σ
1	72.6	14.6	14.45	0.758565	0.000019
2	30.8	7.56	11.85	0.750505	0.000012
3	31.2	6.02	15.10	0.761392	0.000011
4	22.5	6.02	10.87	0.747459	0.000012
5	37.9	7.59	14.53	0.758846	0.000013
6	19.5	5.11	11.09	0.748270	0.000015
4	20.2	4.43	13.27	0.754990	0.000016

Fig DR1. Rb-Sr isochron age of the phlogopites from the Kimberlite in the North Korea

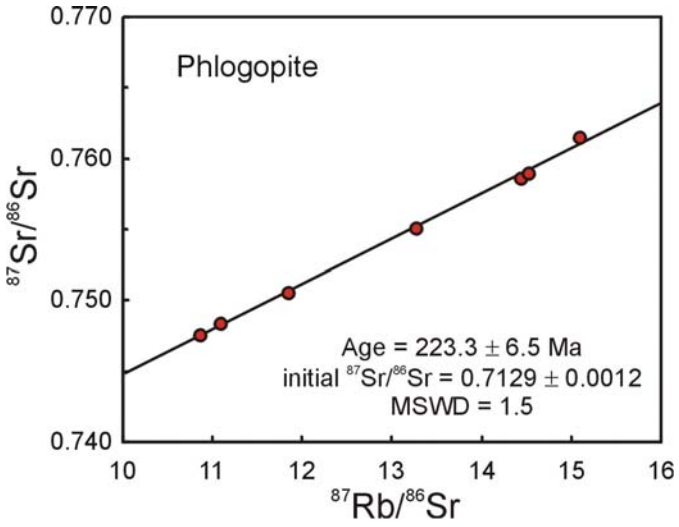

Table DR2. $^{40}Ar/^{39}Ar$ data of whole rock for Cenozoic basalt

t (°C)	^{36}Ar	^{37}Ar	^{38}Ar	^{39}Ar	^{40}Ar	$^{39}Ar/^{40}Ar$	$^{36}Ar/^{40}Ar$	^{39}Ar (%)	Age (Ma)	2 σ
760	0.000046	0.001012	0.000045	0.001302	0.001509	0.08650	0.003045	0.18	13.37	4.75
840	0.000621	0.008471	0.000014	0.031813	0.018254	0.15778	0.003078	4.39	6.63	1.71
880	0.000440	0.006659	0.000014	0.031541	0.016909	0.21465	0.002995	4.35	6.20	1.34
920	0.003363	0.019714	0.000030	0.097440	0.056278	0.09280	0.003203	13.43	6.68	2.85
950	0.000499	0.028109	0.000042	0.114276	0.065208	0.53757	0.002346	15.75	6.59	0.38
980	0.000067	0.027853	0.000030	0.075234	0.042926	1.20069	0.001066	10.37	6.59	0.11
1020	0.000081	0.033481	0.000023	0.050653	0.028988	0.95961	0.001526	6.98	6.61	0.17
1060	0.000150	0.030223	0.000022	0.031419	0.016786	0.51479	0.002453	4.33	6.18	0.45
1100	0.000079	0.031229	0.000020	0.030565	0.017463	0.75174	0.001931	4.21	6.60	0.29

1150	0.000061	0.034676	0.000036	0.033670	0.019175	0.90517	0.001640	4.64	6.58	0.22
1220	0.000169	0.070235	0.000067	0.067539	0.038761	0.76120	0.001906	9.31	6.63	0.25
1300	0.000437	0.753737	0.000171	0.114601	0.067974	0.58103	0.002218	15.80	6.85	0.50
1370	0.000082	0.143441	0.000046	0.020731	0.012254	0.56767	0.002249	2.86	6.83	0.52
1450	0.000146	0.189864	0.000055	0.024558	0.015257	0.42014	0.002501	3.39	7.18	0.84

J = 0.0064030 ± 0.0000160

Plateau Age = 6.60 ± 0.15 Ma, MSWD = 0.65, includes 99.82% of the 39Ar

Isochron Age = 6.60 +/- 0.11 Ma, 40Ar/36Ar = 295.5 +/ 3.7, MSWD = 0.71

Fig DR2. Plateau diagram for the Cenozoic basalt

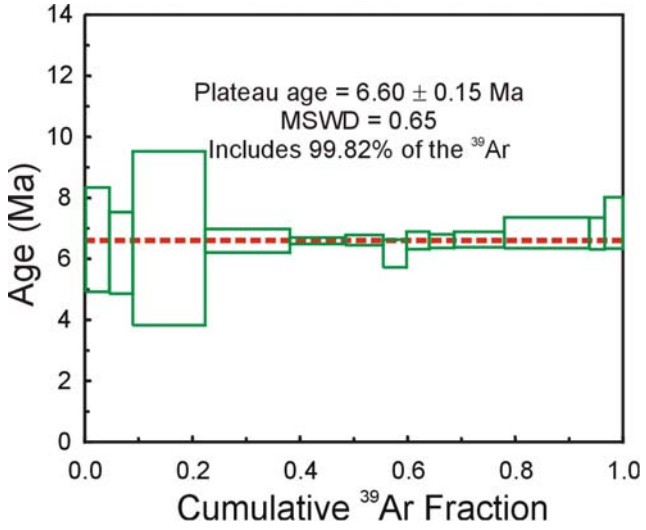

Table DR3. Geochemical and Sr-Nd-Hf isotopic data of Triassic kimberlites from the North Korea

Sample	05NK38	05NK39	Sample	05NK38	05NK39
SiO_2 (wt%)	47.69	45.53	t (Ma)	223	223
TiO_2	0.84	0.88	Rb (ppm)	234	218
Al_2O_3	9.94	9.45	Sr (ppm)	1097	994
TFe_2O_3	8.23	8.73	$^{87}Rb/^{86}Sr$	0.6164	0.6363
MnO	0.10	0.10	$^{87}Sr/^{86}Sr$	0.715121	0.715108
MgO	12.58	12.65	2σ	0.000013	0.000011
CaO	7.54	8.61	$^{87}Sr/^{86}Sr_i$	0.713148	0.713072
Na_2O	1.04	0.44	Sm (ppm)	14.3	14.3
K_2O	4.87	4.35	Nd (ppm)	86.9	86.5
P_2O_5	0.93	0.90	$^{147}Sm/^{144}Nd$	0.0992	0.0998
LOI	5.61	7.67	$^{143}Nd/^{144}Nd$	0.511462	0.511445
TOTAL	99.38	99.31	2σ	0.000013	0.000012
Mg#	75.3	74.3	$\varepsilon_{Nd}(0)$	-22.9	-23.3
Li (ppm)	32	37	$\varepsilon_{Nd}(225)$	-20.2	-20.5
Be	4.3	3.8	$T_{DM}(Nd)$	2126	2158
Sc	18	19	$f_{Sm/Nd}$	-0.50	-0.49
V	113	125	Lu (ppm)	0.22	0.20
Cr	928	1019	Hf (ppm)	4.3	4.6

Co	46	48
Ni	388	424
Cu	43	53
Zn	96	107
Ga	15	15
Rb	230	221
Sr	1041	969
Y	23	25
Zr	219	249
Nb	13	11
Cd	0.036	0.045
Cs	20	28
Ba	3449	3438
La	98.5	105
Ce	193	205
Pr	23.8	25.0
Nd	91.0	93.7
Sm	14.6	15.3
Eu	3.6	3.7
Gd	10.0	10.5
Tb	1.06	1.13
Dy	4.78	5.03
Ho	0.86	0.91
Er	2.01	2.13
Tm	0.28	0.29
Yb	1.79	1.81
Lu	0.25	0.26
Hf	4.95	5.69
Ta	0.65	0.53
Pb	15.2	30.8
Th	16.8	23.5
U	1.99	2.07

$^{176}Lu/^{177}Hf$	0.0071	0.0061
$^{176}Hf/^{177}Hf$	0.281916	0.281904
2σ	0.000008	0.000009
$^{176}Hf/^{177}Hf_i$	0.281886	0.281878
$\varepsilon Hf(t)$	-26.4	-26.7
$T_{DM}(Hf)$	2237	2187
$f_{Lu/Hf}$	-0.79	-0.82

Fig. DR3. Chondrite-normalized REE patterns and Primitive Mantle (PM)-normalized trace element patterns of the kimberlites in the North Korea

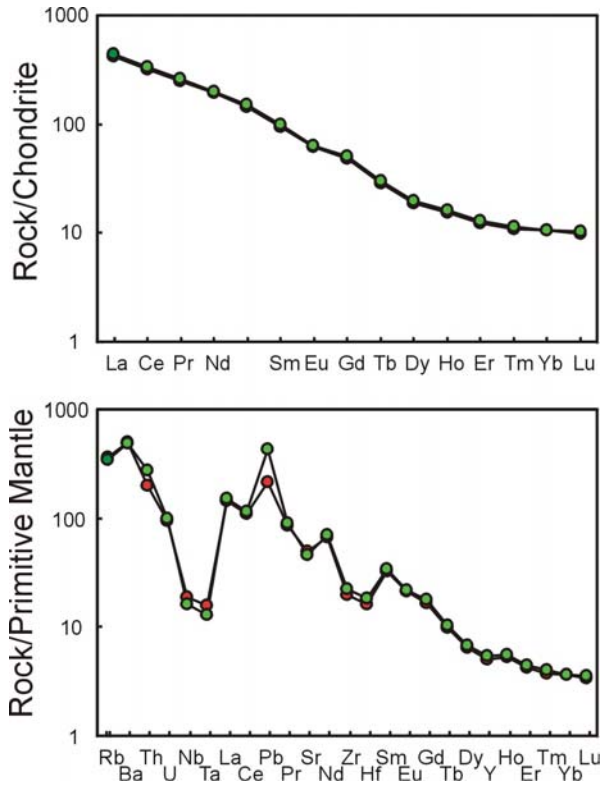

Table DR4. Mineral components of xenoliths in the Triassic kimberlites and Cenozoic basalt from the North Korea

Sample	Min	SiO_2	TiO_2	Al_2O_3	Cr_2O_3	FeO	MnO	MgO	CaO	Na_2O	K_2O	NiO	Total	Fo%	Cr#
05NK41	Ol	41.01	0.00	0.04	0.03	10.66	0.15	48.40	0.09	0.01	0.00	0.38	100.78	89	
05NK42	Ol	41.61	0.00	0.01	0.01	9.08	0.13	49.07	0.04	0.00	0.00	0.41	100.04	91	
05NK43	Ol	41.29	0.00	0.03	0.02	9.94	0.15	49.16	0.08	0.01	0.00	0.40	101.11	90	
05NK44	Ol	41.08	0.00	0.04	0.02	10.43	0.15	48.40	0.10	0.02	0.01	0.39	100.64	89	
05NK45	Ol	40.38	0.00	0.03	0.02	9.94	0.15	48.53	0.08	0.01	0.00	0.37	99.50	90	
05NK46	Ol	41.14	0.01	0.03	0.02	10.32	0.15	48.67	0.08	0.02	0.01	0.39	100.82	89	
05NK47	Ol	41.38	0.01	0.01	0.01	9.20	0.13	48.41	0.06	0.00	0.00		99.22	90	
05NK49	Ol	41.19	0.00	0.03	0.01	10.27	0.15	48.22	0.08	0.02	0.00	0.36	100.34	89	
05NK41	Opx	55.03	0.16	5.16	0.40	6.80	0.15	32.29	0.84	0.15	0.00	0.10	101.07		
05NK42	Opx	55.70	0.08	4.28	0.44	6.02	0.15	33.41	0.66	0.08	0.01	0.10	100.94		
05NK43	Opx	54.69	0.10	5.12	0.47	6.35	0.14	32.32	0.92	0.18	0.01	0.12	100.43		
05NK44	Opx	54.64	0.16	5.52	0.40	6.57	0.14	32.10	1.01	0.18	0.00	0.11	100.84		
05NK45	Opx	54.15	0.15	5.05	0.39	6.33	0.14	32.10	0.89	0.15	0.01	0.11	99.48		
05NK46	Opx	54.70	0.16	5.34	0.39	6.48	0.14	32.19	0.92	0.16	0.01	0.10	100.60		
05NK47	Opx	55.28	0.11	4.84	0.49	6.18	0.14	32.79	0.91	0.13	0.00	0.11	100.98		
05NK48	Opx	54.90	0.14	5.26	0.44	6.34	0.13	32.40	0.91	0.15	0.01	0.10	100.77		
05NK49	Opx	54.49	0.17	5.30	0.39	6.32	0.14	32.25	0.88	0.16	0.00	0.11	100.22		
05NK50	Opx	53.46	0.14	5.39	0.50	6.19	0.14	30.53	1.10	0.15	0.01		97.61		

05NK41	Cpx	51.98	0.63	7.31	0.76	3.38	0.10	15.05	19.11	1.91	0.01	0.05	100.30		
05NK42	Cpx	52.58	0.31	5.96	0.92	2.55	0.09	15.42	20.66	1.56	0.01	0.05	100.10		
05NK43	Cpx	52.21	0.43	7.02	0.93	3.22	0.09	15.55	18.66	1.92	0.01	0.05	100.08		
05NK44	Cpx	51.89	0.57	7.47	0.76	3.38	0.10	15.54	18.63	1.73	0.01	0.05	100.15		
05NK45	Cpx	51.47	0.58	7.08	0.78	3.11	0.10	15.17	19.21	1.72	0.01	0.05	99.29		
05NK46	Cpx	51.91	0.60	7.42	0.74	3.17	0.10	15.41	19.14	1.82	0.01	0.06	100.38		
05NK47	Cpx	52.45	0.39	6.54	0.95	2.97	0.08	15.70	19.68	1.62	0.01	0.05	100.44		
05NK48	Cpx	52.03	0.51	7.05	0.82	3.10	0.08	15.50	19.22	1.72	0.01	0.04	100.09		
05NK49	Cpx	51.70	0.62	7.42	0.77	3.18	0.09	15.34	19.08	1.80	0.01	0.05	100.06		
05NK50	Cpx	51.74	0.48	7.08	0.86	3.60	0.10	15.96	18.65	1.52	0.01	0.05	100.04		
05NK41	Sp	0.10	0.19	56.50	9.59	11.87	0.11	20.05	0.01	0.01	0.00	0.36	98.95		38
05NK42	Sp	0.05	0.09	53.63	13.42	10.59	0.00	20.55	0.01	0.01	0.00	0.38	98.75		49
05NK43	Sp	0.10	0.16	54.44	11.89	11.34	0.13	20.14	0.01	0.00	0.00	0.37	98.71		45
05NK44	Sp	0.09	0.21	56.88	9.89	11.12	0.11	20.32	0.00	0.00	0.00	0.37	99.13		41
05NK45	Sp	0.08	0.18	56.46	9.57	10.89	0.11	20.06	0.00	0.00	0.00	0.34	97.84		40
05NK46	Sp	0.07	0.18	56.63	9.78	10.98	0.12	20.11	0.00	0.00	0.00	0.37	98.38		41
05NK47	Sp	0.06	0.15	53.28	13.79	10.72	0.09	20.62	0.01	0.01	0.01	0.39	98.83		50
05NK48	Sp	0.06	0.16	56.38	10.86	10.34	0.12	20.95	0.00	0.01	0.00		98.89		45
05NK49	Sp	0.09	0.19	57.21	9.33	10.88	0.11	20.43	0.01	0.00	0.00	0.36	98.76		40
05NK50	Sp	0.12	0.23	53.99	12.20	11.50	0.13	20.36	0.00	0.01	0.00	0.34	98.60		45
JB3-1	Ol	41.33	0.01	0.00	0.00	10.47	0.17	48.82	0.02	0.01	0.00	0.39	101.21	89	
JB3-2	Ol	41.88	0.00	0.01	0.01	9.38	0.16	49.74	0.04	0.01	0.01	0.36	101.58	90	
JB3-3	Ol	41.69	0.00	0.00	0.01	9.10	0.13	49.71	0.05	0.01	0.01	0.38	101.09	91	
JB3-4	Ol	41.19	0.00	0.00	0.02	10.33	0.16	48.97	0.03	0.01	0.00	0.39	101.11	89	
JB3-5	Ol	41.56	0.01	0.00	0.00	8.65	0.13	50.30	0.03	0.01	0.00	0.38	101.07	91	
JB3-6	Ol	41.24	0.00	0.00	0.02	8.71	0.15	50.03	0.04	0.00	0.01	0.37	100.59	91	
JB3-1	Opx	55.62	0.10	4.14	0.23	6.52	0.17	32.83	0.49	0.08	0.00	0.10	100.29		
JB3-2	Opx	56.54	0.07	3.62	0.45	5.92	0.14	33.45	0.54	0.07	0.01	0.10	100.89		
JB3-3	Opx	56.60	0.00	3.65	0.45	5.79	0.17	33.56	0.74	0.03	0.00	0.11	101.11		
JB3-4	Opx	56.14	0.10	4.16	0.27	6.52	0.18	33.04	0.49	0.08	0.01	0.13	101.13		
JB3-5	Opx	57.11	0.06	2.44	0.48	5.48	0.16	34.49	0.57	0.04	0.00	0.11	100.96		
JB3-6	Opx	56.90	0.02	2.35	0.46	5.46	0.17	34.20	0.60	0.06	0.00	0.10	100.31		
JB3-1	Cpx	52.81	0.54	7.00	0.69	2.65	0.07	14.38	20.15	2.05	0.00	0.05	100.40		
JB3-2	Cpx	53.73	0.37	5.65	1.16	2.41	0.07	15.23	20.57	1.79	0.01	0.03	101.02		
JB3-3	Cpx	53.69	0.08	3.62	0.66	2.47	0.09	17.06	22.42	0.46	0.00	0.07	100.62		
JB3-4	Cpx	53.33	0.57	6.90	0.65	2.51	0.10	14.42	20.05	2.10	0.01	0.02	100.66		
JB3-5	Cpx	53.74	0.17	3.45	1.28	2.21	0.09	16.31	21.60	1.08	0.01	0.03	99.97		
JB3-6	Cpx	53.56	0.06	3.06	1.06	2.21	0.08	16.60	21.94	1.00	0.01	0.03	99.60		
JB3-1	Sp	0.01	0.06	59.76	8.22	10.32	0.11	20.90	0.00	0.00	0.00	0.40	99.78		8.8
JB3-2	Sp	0.03	0.12	50.00	18.46	11.44	0.12	19.65	0.00	0.01	0.00	0.27	100.10		20
JB3-3	Sp	0.04	0.04	48.89	19.00	11.78	0.15	19.71	0.00	0.01	0.00	0.32	99.93		21
JB3-4	Sp	0.03	0.04	59.33	8.11	10.25	0.14	20.62	0.00	0.00	0.00	0.37	98.92		8.8
JB3-5	Sp	0.03	0.16	36.15	33.57	12.46	0.17	17.66	0.00	0.00	0.00	0.18	100.37		38
JB3-6	Sp	0.04	0.09	34.36	34.63	13.45	0.23	17.05	0.00	0.01	0.01	0.20	100.07		40

Fig. DR4. Comparison of the olivine Mg# of the peridotite xenoliths from mid-Ordovician and Late Triassic kimberlites and Cenozoic alkaline basalts in the east Sino-Korean Craton. Data for xenoliths from Triassic kimberlites and Cenozoic basalts in North Korea are from this work; other data from Zheng et al., 2007 and references therein

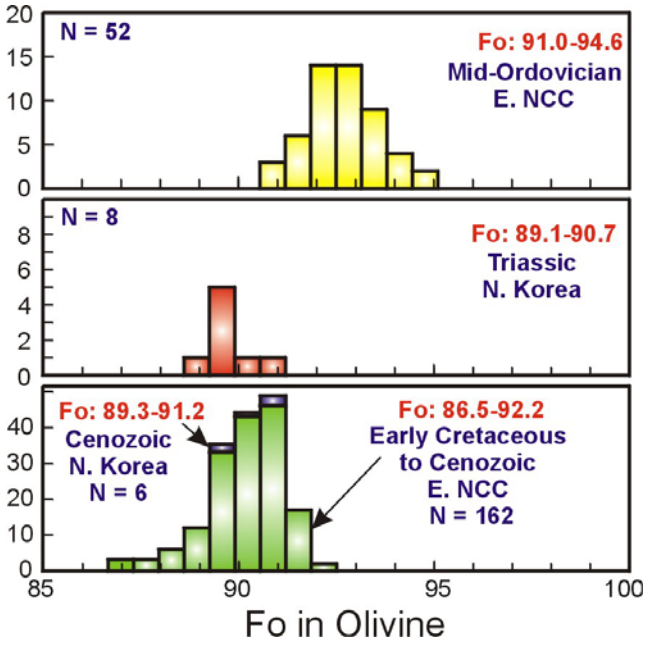

Table DR5. The equilibrium temperatures of the xenoliths in the Triassic kimberlites and Cenozoic basalts from the North Korea

	Temperatures (T °C)			
	[SS81]	[BK Ca in opx @ 15 kBar]	[WES91 - opx-spinel]	[WES91 - Cr-Al-opx]
05NK41	1069	1009	1013	**1010**
05NK42	991	954	958	**991**
05NK43	1076	1034	1041	**1041**
05NK44	1095	1057	1044	**1026**
05NK45	1062	1026	1004	**1009**
05NK46	1081	1031	1027	**1016**
05NK47	1050	1028	1025	**1033**
05NK48	1075	1029	1029	**1033**
05NK49	1073	1023	1015	**1017**
05NK50	1110	1087	1086	**1077**
JB3-1	951	891	880	**904**
JB3-2	947	910	940	**965**
JB3-3	958	978	954	**965**
JB3-4	951	891	879	**918**
JB3-5	899	919	895	**927**
JB3-6	911	932	903	**919**

References*:*

Sachtleben, T., Seck, H. A. Chemical control of Al-solubility in orthopyroxene and its implications on pyroxene geothermometry. Contrib. Mineral. Petrol. 78, 157–165 (1981).

Brey, G.P., Kohler, T. Geothermobarometry in four-phase lherzolites (II): new thermobarometers and practical assessment of existing thermobarometers. J. Petrol. 31, 1353–1378 (1990).

Witt-Eickschen, G. E., Seck, H. A. Solubility of Ca and Al in orthopyroxene from spinel peridotite: an improved version of an empirical geothermometer. Contrib. Mineral. Petrol. 106, 431–439 (1991).

Table DR6. In-situ platinum-group element (PGE) concentrations (ppm) of sulfides in the peridotites from the Triassic kimberlites

No.	Os	Ir	Ru	Pt	Pd	Re
41S01	14.18	21.54	17.62	6.35	23.11	-
41S06	13.14	19.10	14.01	1.84	9.27	-
43S01	9.45	10.20	10.58	5.31	23.80	32.75
43S06	3.71	4.51	4.72	4.63	15.53	13.50
43S07	8.37	8.59	8.87	2.52	8.67	21.00
43S08	6.53	5.93	5.87	3.10	3.85	12.50
43S09	1.80	1.92	2.15	4.21	6.44	6.75
43S10	7.31	8.84	7.99	7.73	11.13	12.50
43S11	12.53	17.38	16.13	10.95	91.31	31.50
45S01	15.04	18.02	15.48	5.67	13.65	135.25
45S02	15.71	14.48	20.73	12.71	28.80	-
45S03	10.12	14.42	10.82	6.63	11.25	-
45S05	4.16	5.38	8.14	1.06	5.91	-
45S06	47.78	47.41	55.27	14.39	47.51	-
45S07	29.27	33.32	32.46	18.91	38.42	--
49S01	0.95	0.80	0.67	0.15	0.74	0.04
49S02	7.82	10.29	11.45	13.73	70.96	0.38
49S03	11.12	12.73	16.89	1.42	16.51	0.98
49S04	26.69	23.47	30.54	2.06	20.53	1.80
49S07	14.49	14.62	16.01	0.33	4.04	1.58
49S07-2	12.24	15.78	15.28	0.44	6.33	1.35
49S08	14.51	13.98	16.73	0.40	1.75	2.35
49S09	17.20	20.62	16.76	1.07	6.85	0.85
49S10	10.65	9.32	10.32	2.40	7.62	1.00
49S12	3.61	5.47	4.65	3.28	20.65	1.00
49S12-2	4.76	7.23	6.11	3.55	23.78	1.38
49S14	42.27	38.95	37.35	0.29	1.37	2.18
49S15	27.96	31.56	29.45	11.02	21.33	2.65
49S15-2	38.69	38.53	37.56	1.12	7.84	3.75

Table DR7. Platinum-group element concentrations and Re-Os isotopic data of peridotites from the Triassic kimberlites (05NK41 to 50) and Cenozoic basalts (JB3-1 to 3-6) in the North Korea

Sample	Rock type	Fo%	Cr%	Re	Os	Ir	Ru	Pt	Pd	$^{187}Re/^{188}Os$	$^{187}Os/^{188}Os$
05 NK 41	**Peridotite**	89	38	0.219	3.542	2.646	5.350	5.467	4.685	0.298	0.12584
05 NK 42	**Peridotite**	90	49	0.012	2.120	4.053	7.971	7.873	6.473	0.026	0.12792
05 NK 43	**Peridotite**	90	45	0.298	3.123	2.485	5.476	9.002	9.909	0.460	0.12946
05 NK 44	**Peridotite**	89	41	0.011	3.658	4.034	8.030	6.916	5.675	0.014	0.12804
05 NK 45	**Peridotite**	90	40	0.127	2.468	3.020	6.055	5.578	4.921	0.248	0.12601
05 NK 46	**Peridotite**	90	41	0.040	3.522	3.222	6.519	6.147	5.503	0.055	0.12612
05 NK 47	**Peridotite**	90	50	0.013	3.922	3.141	6.144	5.824	4.074	0.016	0.12448
05 NK 48	**Peridotite**	-	45	0.004	2.723	3.474	6.573	6.322	3.937	0.008	0.12552
05 NK 49	**Peridotite**	89	40	0.098	5.277	2.607	5.382	5.325	4.917	0.089	0.12677
05 NK 50	**Peridotite**	-	45	0.006	2.842	3.873	7.604	6.662	4.491	0.010	0.12575
JB3-1	**Peridotite**	89	8.8	0.039	5.84	4.193	12.254	6.333	-	0.032	0.12619
JB3-2	**Peridotite**	90	20	0.016	1.34	1.595	3.346	3.551	-	0.057	0.12187
JB3-3	**Peridotite**	91	21	0.040	1.61	1.668	5.091	4.801	-	0.120	0.12603
JB3-4	**Peridotite**	89	8.8	0.078	2.34	2.572	4.823	4.732	-	0.161	0.12723
JB3-5	**Peridotite**	91	38	0.047	1.73	2.564	4.731	4.491	-	0.131	0.12439
JB3-6	**Peridotite**	91	40	0.010	2.18	1.814	4.896	2.906	-	0.023	0.12765

Table DR8. In-situ Re-Os isotopic data of sulfides in the peridotites from the Triassic kimberlites

Sample No	$^{187}Re/^{188}Os$	1σ	$^{187}Os/^{188}Os$	1σ	Initial Os ratio	γOs(t)
05NK41 s02	0.7809	0.0250	0.13713	0.00086	0.13426	7.03
05NK41 s03	0.4216	0.0068	0.13314	0.00032	0.13159	4.83
05NK41 s04	0.0663	0.0013	0.12362	0.00068	0.12338	-1.62
05NK41 s07	2.5138	0.0330	0.16359	0.00089	0.15435	22.98
05NK41bs00	1.1915	0.0180	0.12046	0.00080	0.11608	-7.48
05NK41bs01	0.5975	0.0069	0.11802	0.00091	0.11582	-7.66
05NK41bs07	0.6718	0.0260	0.12550	0.00050	0.12303	-1.92
05NK43 s04	1.1388	0.0160	0.13215	0.00087	0.12797	2.00
05NK43bs09	0.3430	0.0042	0.12805	0.00030	0.12679	1.09
05NK43bs13	0.4290	0.0065	0.12999	0.00072	0.12842	2.38
05NK45 s05	0.5660	0.0046	0.13663	0.00061	0.13455	7.27
05NK45 s09	0.3324	0.0045	0.13224	0.00081	0.13102	4.46
05NK45bs02	0.4544	0.0027	0.12517	0.00044	0.12350	-1.54
05NK45bs04	0.1089	0.0006	0.12504	0.00039	0.12464	-0.62
05NK46 bs01	0.0937	0.0040	0.12584	0.00018	0.12550	0.07
05NK46 bs02	0.0161	0.0010	0.12691	0.00034	0.12685	1.15
05NK46 bs03	0.0121	0.0002	0.12272	0.00022	0.12268	-2.18
05NK46 s05	0.4068	0.0060	0.13502	0.00081	0.13353	6.46
05NK46 s06	0.0267	0.0004	0.12388	0.00025	0.12378	-1.30
05NK46 s07	0.0321	0.0002	0.12466	0.00013	0.12454	-0.69
05NK49 bs00	0.1924	0.0016	0.12832	0.00061	0.12761	1.75
05NK49 bs01	0.2956	0.0037	0.12635	0.00029	0.12526	-0.13
05NK49 bs03	0.1636	0.0065	0.12846	0.00064	0.12786	1.95
05NK49 bs04a	0.5915	0.0041	0.12620	0.00052	0.12403	-0.65

05NK49 bs04b	0.6739	0.0085	0.12453	0.00033	0.12206	-2.70
05NK49 bs07	0.3573	0.0029	0.12466	0.00073	0.12335	-1.65
05NK49 bs08	0.3568	0.0098	0.12985	0.00063	0.12854	2.48
05NK49 bs10	0.4693	0.0085	0.13017	0.00058	0.12845	2.41
05NK49 s05	1.0354	0.0130	0.14066	0.00074	0.13686	9.09
05NK49 s07	0.3903	0.0067	0.13381	0.00090	0.13238	5.54
05NK41 s02	0.7809	0.0250	0.13713	0.00086	0.13426	7.03
05NK41 s03	0.4216	0.0068	0.13314	0.00032	0.13159	4.83
05NK41 s04	0.0663	0.0013	0.12362	0.00068	0.12338	-1.62
05NK41 s07	2.5138	0.0330	0.16359	0.00089	0.15435	22.98

Table DR9. Sr-Nd-Hf isotopic data of the clinopyroxenes in the peridotites from the Triassic kimberlites

Sam. No.	Rb	Sr	$^{87}Rb/^{86}Sr$	$^{87}Sr/^{86}Sr$	2σ	$^{87}Sr/^{86}Sr_i$
05NK41	0.038	119	0.0009	0.703349	0.000015	0.70335
05NK41*			*0.0009*	**0.703289**	**0.000012**	0.70329
05NK42	0.006	31.2	0.0005	0.702455	0.000012	0.70245
05NK43	0.034	121	0.0008	0.703814	0.000013	0.70381
05NK44	0.028	63.3	0.0013	0.702602	0.000013	0.70260
05NK44*				**0.702586**	**0.000023**	
05NK45	0.053	65.4	0.0024	0.703360	0.000013	0.70335
05NK45*			*0.0024*	**0.703336**	**0.000010**	
05NK46	0.031	68.0	0.0013	0.703319	0.000012	0.70331
05NK46*				**0.702579**	**0.000013**	
05NK47	0.082	65.5		0.704074	0.000014	0.70406
05NK48	0.057	90.5	0.0018	0.703185	0.000012	0.70318
05NK48*				**0.703107**	**0.000011**	
05NK49	0.067	69.8	0.0028	0.703115	0.000013	0.70311
05NK49*				**0.703103**	**0.000011**	
05NK50	0.008	60.6	0.0004	0.702944	0.000013	0.70294

Sam. No.	Sm	Nd	$^{147}Sm/^{144}Nd$	$^{143}Nd/^{144}Nd$	2σ	$\varepsilon_{Nd}(0)$	$\varepsilon_{Nd}(225Ma)$	$T_{DM}(Nd)$	$f_{Sm/Nd}$
05NK41	1.28	4.24	0.1829	0.513047	0.000033	8.0	8.4	-4	-0.07
05NK41*	1.79	5.78	0.1877	0.513053	0.000015	8.1	8.4	-3	-0.05
05NK42	0.53	1.24	0.2594	0.513717	0.000021	21.1	19.3	87	0.32
05NK43	1.12	4.76	0.1428	0.512919	0.000018	5.5	7.0	-8	-0.27
05NK44	1.06	2.71	0.2369	0.513269	0.000026	12.3	11.2	7	0.20
05NK44*	1.44	3.71	0.2352	0.513253	0.000017	12.0	10.9	5	0.20
05NK45	1.01	2.38	0.2567	0.513218	0.000093	11.3	9.6	5	0.30
05NK45*	1.22	2.93	0.2520	0.513206	0.000015	11.1	9.5	3	0.28
05NK46	1.05	2.74	0.2310	0.513365	0.000127	14.2	13.2	13	0.17
05NK46*	1.33	3.53	0.2276	0.513321	0.000016	13.3	12.5	8	0.16
05NK47	0.88	2.43	0.2195	0.513013	0.000012	7.3	6.7	-10	0.12
05NK48	1.57	4.27	0.2216	0.513129	0.000015	9.6	8.9	-1	0.13
05NK49	1.73	4.42	0.2373	0.513296	0.000013	12.8	11.7	5	0.21
05NK50	1.03	2.78	0.2236	0.513226	0.000048	11.5	10.7	5	0.14

Sam. No.	Lu	Hf	$^{176}Lu/^{177}Hf$	$^{176}Hf/^{177}Hf$	2σ	$\varepsilon_{Hf}(0)$	$\varepsilon_{Hf}(225Ma)$	$T_{DM}(Hf)$	$f_{Lu/Hf}$
05NK41	0.14	0.88	0.0215	0.283196	0.000007	15.0	16.6	171	-0.35
05NK41*				**0.283174**	**0.000002**				
05NK42	0.11	0.34	0.0468	0.284715	0.000016	68.7	66.6	8590	0.41
05NK42*				**0.284738**	**0.000006**				
05NK43	0.14	0.58	0.0342	0.283377	0.000010	21.4	21.2	-1649	0.03
05NK44	0.16	0.81	0.0282	0.283317	0.000010	19.3	19.9	-354	-0.15
05NK44*				**0.283311**	**0.000003**				

05NK45	0.14	0.64	0.0311	0.283267	0.000010	17.5	17.7	-124	-0.06
05NK45*				**0.283268**	**0.000004**				
05NK46	0.16	0.78	0.0275	0.283325	0.000013	19.6	20.3	-372	-0.17
05NK46*				**0.283321**	**0.000004**				
05NK46*				**0.283314**	**0.000003**				
05NK47	0.12	0.59	0.0287	0.283392	0.000015	21.9	22.5	-785	-0.14
05NK48	0.12	0.69	0.0233	0.283308	0.000011	18.9	20.3	-206	-0.30
05NK48*				**0.283279**	**0.000004**				
05NK49	0.14	0.79	0.0245	0.283267	0.000012	17.5	18.7	-65	-0.26
05NK49*				**0.283248**	**0.000003**				
05NK50	0.09	0.60	0.0217	0.283428	0.000017	23.2	24.8	-574	-0.35

***: duplicate analyses; the bold data are unspiked**

Rb, Sr, Sm, Nd, Lu and Hf (ppm)